Intrinsic Mobility of a Dissociated Dislocation in Silicon

Wei Cai,[1] Vasily V. Bulatov,[1,2] João F. Justo,[3] Ali S. Argon,[1] and Sidney Yip[1]
[1]*Massachusetts Institute of Technology, Cambridge, Massachusetts 02139*
[2]*Lawrence Livermore National Laboratory, University of California, Livermore, California 94550*
[3]*Instituto de Fisica da Universidade de São Paulo, CP 66318, CEP 05315-970 São Paulo-SP, Brazil*
(Received 11 November 1999)

Dislocation velocities in silicon in the experimental range of temperature and stress are studied *a priori* by combining a mechanistic treatment of elementary kink processes with activation energies obtained by atomistic calculations. Pronounced effects of intrinsic coupling of the dissociated partial dislocations are captured in kinetic Monte Carlo simulations, which are consistent with observed velocity variations with applied stress. As a result, the nature of "weak obstacles" to kink propagation, a long-standing postulate in previous data interpretation, is clarified. A striking new effect is predicted and offered for experimental verification when dislocation velocity shows nonmonotonic oscillatory behavior with increasing stress.

PACS numbers: 61.72.Lk, 61.72.Bb, 61.72.Cc, 62.20.Fe

Covalent bonding in silicon and other semiconductors gives rise to a high barrier to dislocation motion [1,2]. In an attempt to quantify this behavior in terms of the underlying atomistic mechanisms, much theoretical effort has been spent on obtaining accurate activation parameters for kink nucleation and migration. However, despite the recent theoretical progress and a considerable body of experimental observations, how dislocations actually move from one Peierls valley to another under stress is still an open question. The fundamental difficulty is that interpretation of the available data has been hampered by the lack of a theoretical description which is sufficiently free of *ad hoc* assumptions and capable of relating dislocation mobility behavior to the underlying kink mechanisms.

In this work we present such a description by adopting a kinetic Monte Carlo (kMC) treatment of kink nucleation, migration, and annihilation processes along with full elastic interactions between the dissociated partial dislocations. The formulation is designed to produce the overall dislocation movement as the cumulative effect of a large number of individual kink events, requiring for input only the kink formation and migration energies available from atomistic calculations [3–8]. In focusing on the stress dependence of dislocation velocity, we show that it is strongly affected by the compatibility between the averaged separation between the partials X_0 and the period of the Peierls barrier. When the two are commensurate (integral X_0), the dislocation mobility is low at low stress and increases superlinearly below a critical stress value. In the case when X_0 is half-integral, no threshold behavior is observed and the velocity is essentially linear in the stress. Both types of variations have been observed experimentally. Previous attempts to rationalize the threshold behavior have resulted in the postulate of a random distribution of weak obstacles or "dragging points" on the dislocation line [9–11], a notion which we are able to clarify with the present description.

Our model deals with a screw dislocation $(a/2)[1\bar{1}0]$ dissociated into two 30° partials in the (111) plane. Each partial is represented by a piecewise straight line composed of alternating horizontal (H) and vertical (V) segments. The length of H segments can be any multiple of b, while the V segments are all of the same length, the kink height h. The stacking fault bounded by the two parallel partials has a width measured in multiples of h. The simulation cell is oriented with the partials running horizontally so that a periodic boundary condition can be applied in this direction. The horizontal and vertical directions are labeled z and x, respectively. The dislocation glides in the vertical direction, upward being along $\langle 11\bar{2}\rangle$, as a result of comigration of the two partials which in turn follows from the elementary kink events.

In each simulation step, a stochastic sampling is carried out to determine which event will take place next: a kink pair nucleation on the H segments in the upward (downward) direction or a kink (V segment) translation to the left (right) by an amount b. The rates of these elementary events are calculated based on the energetics of the corresponding kink mechanisms. For example, for a kink pair nucleation mechanism three energy terms are considered: a formation energy obtained by relaxing the atomic configuration of the kink pair using an empirical potential or first principles methods, an energy bias which favors the reduction of the stacking-fault area, and the elastic interaction between a given segment and all the other segments and applied stress (so-called Peach-Koehler interaction). Accordingly, the nucleation rate for an embryonic kink pair (width one b) on a partial with Burgers vector $\vec{b}_p$ and under stress σ_{ij} is calculated as

$$j_{kp}(1) = \omega_0 \exp\left(-\frac{E_{kp}(1) + (\pm\gamma_{\mathrm{SF}} - \sigma_{yz} b_{p,z} - \sigma_{yx} b_{p,x})A/2}{k_B T}\right), \tag{1}$$

 0031-9007/00/84(15)/3346(4)$15.00

where ω_0 is the preexponential "frequency" factor, which we set equal to the *Debye frequency.* γ_{SF} is the stacking fault energy with a "+" or a "−" sign for the leading and trailing partial, respectively. $A = \pm bh$ is the area swept out by the dislocation during kink pair nucleation, with a "+" or a "−" sign for upward or downward nucleation, respectively. The factor of $\frac{1}{2}$ appears because we assume that in the saddle point configuration the dislocation has swept out half of the total area A. k_B is the Boltzmann's constant and T is the temperature. σ_{ij} here represents the sum of external stress and the Peach-Koehler stresses from the other segments. Similar expressions, with appropriate modifications, hold for the kink migration rates. The remaining barrier terms, such as $E_{kp}(1)$ in (1), are imported directly from atomistic simulation data.

In implementing the model just described we observed that, once formed, most of the embryonic kink pairs quickly recombine, wasting a great number of kMC cycles on such irrelevant events. For the sake of computational efficiency, we developed a special numerical procedure to calculate a probability per unit time that an embryonic kink pair formed on a given H segment will survive and expand to a *sustainable* width w_s. In practice, we found $w_s = 10b$ is a reasonable choice at which a good fraction (about 1%–10%) of the fresh kink pairs never recombines and thus contributes to the overall dislocation translation.

As we have emphasized, we will rely on atomistic calculations to provide values for the kink formation and migration energies. It was first found in [4] and then rationalized in [6] that for 30° partials four topologically distinct types of kinks can be distinguished, if one neglects the reconstruction defect and its complexes with the four primary kinks. Table I shows formation (E_k) and migration (W_m) energies for all four kinks obtained using the environment-dependent interatomic potential (EDIP) empirical potential [12] and the tight-binding (TB) approximation [7]. Although kink multiplicity can be readily incorporated into our model, in the present work we opted for a simpler parameter space and set representative values for E_k and W_m as follows. Considering that the greatest contribution to dislocation motion comes from kinks that nucleate and migrate at the fastest rates, the value of E_k is taken as the average of the lowest values for two left (LK, LK′) and two right (RK, RK′) kinks separately, giving $E_k = 0.52$ eV (EDIP) and 0.80 eV (TB). For W_m we choose the lower value from the maximum of (LK, LK′) and of (RK, RK′), giving $W_m = 0.89$ eV (EDIP) and 1.52 eV (TB). Since these are zero-temperature values, we apply them at temperature T by adding $-TS$, with entropy S taken as $3k_B$ [13,14]. This completes the specification of our kMC model.

TABLE I. Formation energies, E_k, and migration barriers, W_m, of kinks on 30° partials in silicon, obtained from atomistic calculations using EDIP and TB, in eV. Underlined values are selected for use in kMC simulation.

	E_k		W_m	
	EDIP	TB	EDIP	TB
LK	<u>0.65</u>	<u>0.35</u>	1.46	<u>1.52</u>
RK	0.72	<u>1.24</u>	0.56	2.03
LK′	1.49	0.76	0.62	1.11
RK′	<u>0.39</u>	1.85	<u>0.89</u>	1.42

The inset in Fig. 1 shows a typical result of the simulation, the instantaneous average positions of the leading and trailing partials of a screw dislocation moving in response to a constant applied stress at a constant temperature. During the 0.15 s interval of simulation, the two partials are seen to maintain roughly constant separation as they advance a distance of some 5.7×10^{-6} cm, giving a predicted velocity of 3.8×10^{-5} cm/s. Dislocation velocities obtained from such simulations at various temperatures using the two sets of atomistic activation energies are shown in Fig. 1, along with two sets of experimental data [15,16]. The velocities given by the two sets of atomistic inputs are seen to differ by some 4 orders of magnitude, bracketing the experiments. An Arrhenius fit of the simulated and the experimental velocity data gives an overall activation energy $Q = 1.31$ eV (EDIP), 2.23 eV (TB), and 2.20 (experimental).

We are cautiously optimistic about the above comparison, considering that we did not include the effects of kink multiplicity and used rather approximate values for the frequency factor and entropy. Of the other material parameters entering the model, kink energetics also remains uncertain despite recent impressive advances in atomistic calculations based on interatomic potentials and, presumably more accurate, TB and density functional theory (DFT) methods. In fact, even the DFT calculations

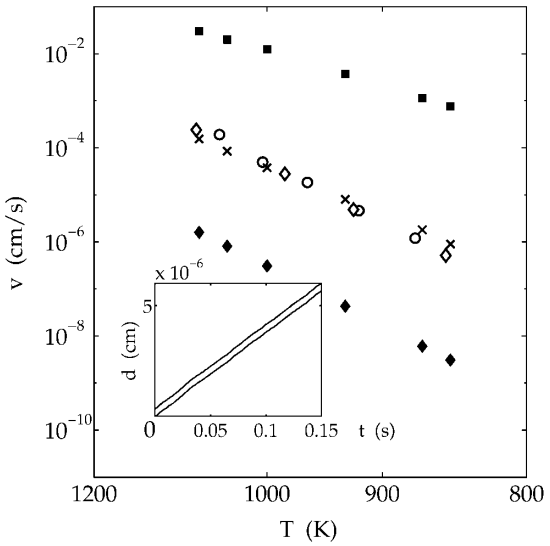

FIG. 1. Temperature-dependent velocities of screw dislocations at stress $\tau = 10$ MPa. Experiments are denoted by ◇ [15] and ○ [16], respectively. ■ and ◆ are kMC predictions using EDIP and TB kink energetics. kMC data for the optimized kink parameters, $E_k = 0.7$ eV and $W_m = 1.2$ eV, are also shown as ×. The inset shows the simulated instantaneous positions of the two partials (see text).

available for the partial dislocations in Si [3,8] have neither converged nor agreed with the experimental estimates which themselves show considerable scatter [17–19]. Despite these uncertainties, the fact that the simulated dislocation velocities bracket the experimental data is significant, indicating that our kMC model is adequate but that the accuracy is limited by the quality of its atomistic input. If and when a more reliable set of atomistic parameters becomes available, the model will be ready to incorporate the new data for more accurate prediction of the intrinsic dislocation mobility in Si. Based on various calculated and experimental estimates available at present, a reasonable set of values to take for (E_k, W_m) would be around $(0.7, 1.2)$. The predicted outcome based on this set is also shown in Fig. 1.

A major goal of this work is to investigate dislocation mobility as a function of applied stress. We have identified two distinct behaviors which warrant detailed analysis. In Fig. 2 we see a threshold behavior where the dislocation velocity is initially low at low stress but increases markedly beyond a certain critical stress τ_c. Although in our simulations this characteristic behavior appears naturally as a result of the underlying kink processes, for its interpretation we follow a simple mechanistic picture proposed in [20] and further developed in [21,22]. We first consider what would be the ideal separation between the two partials if the Peierls barrier were not present. This separation, which we denote as X_0, is given by the expression $X_0 = \mu b^2 \alpha/(\gamma_{\rm SF} - \sigma_{xy} b_x)$, where μ is the shear modulus, $\alpha = [1/4 - 1/12(1 - \nu)]/2\pi$, $b_x = b\sqrt{3}/6$, and ν is the Poisson ratio. The significance of X_0 is that, when it is commensurate with the actual separation X between the partials (in the presence of the Peierls barrier), the two partials are strongly confined to their lowest-energy configuration at the valley of the Peierls potential, and there is significant energy penalty if either one tries to move to the next valley. The only way to avoid this penalty is for the partials to move in unison; since this must require more thermal energy, it follows that, when X_0 is an integral multiple of the period of the Peierls barrier (in this case, h, the kink height), the mobility is low at low stress as seen in Fig. 2. A somewhat weaker threshold behavior is observed experimentally, as indicated also in Fig. 2. This is not unreasonable given that the measurements average over a distribution of local conditions, whereas the prediction is strictly for the case of commensurate barrier (X_0/h is integral). The threshold condition is expected to become ineffective when applied stress becomes high enough for its work to compensate the "commensurate" energy barrier to moving a single partial to the next valley. Based on the numerical parameters used in our simulation, we estimated this critical stress to be $\tau_c = 16.8$ MPa, in agreement with our present kMC simulations and another estimate given in [23].

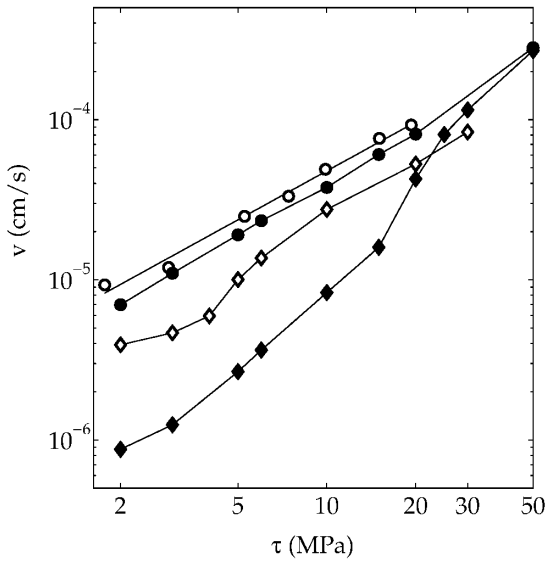

FIG. 2. Velocity of a screw dislocation in Si as a function of stress, at temperature $T = 1000$ K. kMC prediction for a commensurate case ($X_0 = 10.0h$) is shown as ◆, with a "starting stress" at about 20 MPa. Experimental data from [15] shows similar velocity variation, plotted as ◇. kMC results for a noncommensurate case ($X_0 = 10.5h$) are plotted as ●, demonstrating a linear stress-velocity relationship, in agreement with other experiments [16], plotted as ○.

The most common interpretation of the threshold stress variation, long observed, invokes the existence of weak obstacles, assumed to be randomly distributed along the dislocation and having the effect of impeding the kink mobility [9,11,15]. The physical origin of these obstacles has been a long-standing unresolved issue, especially since fitting such models to the experimental data results in rather unreasonable magnitudes for the density of these obstacles [10,11]. Möller was the first to recognize the importance of interaction between the dissociated partials. In his model [10], he attempted to do without *ad hoc* obstacles, but in the end was forced to reintroduce them to account for the low stress mobility variations in Si. In addition to this inconsistency, Möller's model could not resolve another hotly debated experimental controversy. While some researchers have observed very pronounced starting stress behavior [15], others report perfectly linear velocity-stress behavior even down to a very low stress [16] (also shown in Fig. 2). As we have already shown and further discuss below, our kMC model offers a natural resolution.

As demonstrated in the same Fig. 2, when parameter X_0 is a half-integral multiple of h, dislocation velocity increases linearly showing no starting stress behavior. In this case, the lowest-energy dissociated state is doubly degenerate, with $X = X_\pm = X_0 \pm 1/2$. Now each partial can migrate to the adjacent valley without penalty provided the movement occurs in a certain sequence. For $X = X_+$ kink nucleation on the trailing partial can occur more easily since the resulting separation between the nucleated kink and the leading partial becomes X_-. Similarly, for $X = X_-$ nucleation on the leading partial is favored. As a result, when X_0/h is half-integral, there is no commensurate barrier and dislocation mobility should be relatively high, with the two partials moving sequentially through

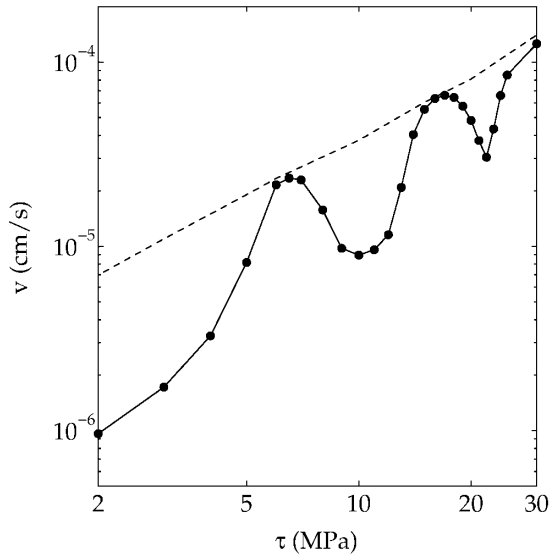

FIG. 3. Dislocation velocity plotted against glide stress σ_{yz}, as ●, predicted for a special case when the ratio of the glide stress σ_{yz} to the nonglide stress σ_{xy} is fixed at -0.16. For comparison, dislocation velocity for a noncommensurate case ($X_0 = 10.5h$) and zero nonglide stress is also shown as the dashed line.

alternate contraction and expansion of the stacking fault. Depending on the value of X_0, one can find either of the two scenarios supported by the experiments: a threshold behavior at low stress (X_0 integral) or a linear variation of the velocity with stress (X_0 half-integral).

For the simulations discussed above, the variation of X_0 was induced by a 5% change in the stacking-fault energy, but a similar effect will manifest by an equivalent variation in the elastic constant, or any other local factor which will influence the dissociation width. In particular, X_0 depends on the so-called nonglide stress, or σ_{xy} in our notation. For an ideal dislocation, this stress component should have no effect on the glide velocity. However, in the context of our present model, σ_{xy} can be used to manipulate the splitting width X_0 and to induce transitions between the "integral" and "half-integral" conditions. A striking illustration of such transitions is presented in Fig. 3, where simulated dislocation velocity is plotted against glide stress σ_{yz} for a special loading condition chosen to maintain a constant ratio -0.16 of glide (σ_{yz}) to nonglide (σ_{xy}) stress components. With increasing stress amplitude, two effects counteract. The increasing glide stress makes both partials move faster while the increasing nonglide stress pushes the partials together making them pass through a sequence of integral and half-integral conditions. Accordingly, the dislocation velocity shows a nonmonotonic oscillatory pattern, each dip corresponding to an integral situation and each hump to a half-integral one.

We conclude by emphasizing that the present work is the first attempt to link the microscopic details being generated by electronic structure and atomistic calculations with dislocation mobility behavior that is directly experimentally accessible. By demonstrating that the experimental velocities measured in Si can be bracketed by two sets of kink activation parameters, we establish the quantitative boundaries on the required accuracy of the future microscopic calculations. In our resolution of the two types of stress variations that have been observed, we show that a consistent theoretical interpretation can result from a mechanistic treatment of dissociated partial dislocations on the basis of elementary kink processes. Finally, we predict a striking new effect of nonmonotonic velocity variations in the low stress regime which we offer for experimental verification.

This work was supported by the NSF MRSEC Program at MIT under Award No. DMR 94-00334 and by the Lawrence Livermore National Laboratory under an ASCI-Level 2 award. V. V. B. acknowledges support from the Office of Basic Energy Sciences, the U.S. Department of Energy. We thank A. George for many helpful discussions. W. C. acknowledges the Manson Benedict Fellowship in Nuclear Engineering.

[1] M. S. Duesbery and G. Y. Richardson, Crit. Rev. Solid State Mater. Sci. **17**, 1 (1991).
[2] J. P. Hirth and J. Lothe, *Theory of Dislocations* (Wiley, New York, 1982), p. 373.
[3] S. Oberg, P. K. Sitch, R. Jones, and M. I. Heggie, Phys. Rev. B **51**, 13 138 (1995).
[4] V. V. Bulatov, S. Yip, and A. S. Argon, Philos. Mag. A **72**, 453 (1995).
[5] R. W. Nunes, J. Bennetto, and D. Vanderbilt, Phys. Rev. Lett. **77**, 1516 (1996).
[6] V. V. Bulatov, J. F. Justo, W. Cai, and S. Yip, Phys. Rev. Lett. **79**, 5042 (1997).
[7] R. W. Nunes, J. Bennetto, and D. Vanderbilt, Phys. Rev. B **57**, 10 388 (1998).
[8] A. Valladares, J. A. White, and A. P. Sutton, Phys. Rev. Lett. **81**, 4903 (1998).
[9] V. Celli, M. Kabler, T. Ninomiya, and R. Thomson, Phys. Rev. **131**, 58 (1963).
[10] H. J. Möller, Acta Metall. **26**, 963 (1978).
[11] H. Alexander, in *Dislocation in Solids*, edited by F. R. N. Nabarro (North-Holland, Amsterdam, 1986), Vol. 7, p. 113.
[12] J. F. Justo, M. Z. Bazant, E. Kaxiras, V. V. Bulatov, and S. Yip, Phys. Rev. B **58**, 2539 (1998).
[13] S. Marklund, Solid State Commun. **54**, 555 (1985).
[14] F. Louchet, Philos. Mag. A **43**, 1289 (1981).
[15] A. George, J. Phys. (Paris) **40**, 133 (1979).
[16] M. Imai and K. Sumino, Philos. Mag. A **47**, 599 (1983).
[17] P. B. Hirsch, A. Ourmazd, and P. Pirouz, Inst. Phys. Conf. Ser. **60**, 29 (1981).
[18] H. Gottschalk, H. Alexander, and V. Dietz, Inst. Phys. Conf. Ser. **87**, 339 (1987).
[19] H. R. Kolar, J. C. H. Spence, and H. Alexander, Phys. Rev. Lett. **77**, 4031 (1996).
[20] W. Benoit, M. Bujard, and G. Gremaud, Phys. Status Solidi A **104**, 427 (1987).
[21] G. Schoeck, Scr. Metall. Mater. **30**, 611 (1994).
[22] F. R. N. Nabarro, Philos. Mag. A **75**, 703 (1997).
[23] Ref. [11], p. 167.